

Synthesis and Characterization of $Sb_{65}Se_{35-x}Ge_x$ Alloys

Saleh Ahmed Saleh

Physics Department, Faculty of Science, Sohag University, Egypt; Physics Department, College of Science & Arts, Najran University, Saudi Arabia.

Email: saleh2010_ahmed@yahoo.com

Received March 16th, 2011; revised April 14th, 2011; accepted April 26th, 2011.

ABSTRACT

Density, chemical, structural and vibrational studies of $Ge_xSb_{65}Se_{35-x}$ system with $0 \leq x \leq 20$ produce by melt-quench technique were carried out using Archimedes method, Energy Dispersive Spectroscopy (EDS), X-ray diffraction (XRD) and Raman spectroscopy. All specimens are polycrystalline in nature as confirmed by XRD pattern. The compositional dependence of the XRD and Raman spectra suggests the presence of two basic structural units, $SbSe_3$ pyramids with three-fold coordinated Sb atom at the apex and $GeSe_4$ tetrahedrons. The compositional dependence of these physico-chemical properties of the investigated samples are investigated and discussed in light of many models.

PACS: 68.55.Ln; 61.50.Ks; 68.55.Jk

Keywords: Ge Doping, Sb_2Se , Structure, Raman Spectroscopy, Chalcogenides

1. Introduction

Chalcogenide alloys (which contain at least one of the chalcogen elements: sulphur, selenium or tellurium) are of special interest due to their wide application in modern electronics, optoelectronics, integrated optics, electrophotography, solar cells, electrical and optical memory devices, among others. One of the recent applications of these chalcogenides is in rewritable optical data recording (phase change recording). This technology is based on reversible phase transition between crystalline and amorphous state. Currently, the primary materials for phase change recording are based on Sb-Te alloys [1-9], but materials research still continues due to the need for increased storage capacity and data recording rates. Nowadays, the attention is extended over Sb-Se system as possible candidates for these applications. Recently the author group has synthesized ternary selenide glasses based on Sb-Se system with addition of Ge, and has considered the basic optical parameters in dependence of glass composition [10]. However, normally the eutectic Sb-Se material system has poor stability, which requires improvement of the stability by doping other elements such as Ge. The higher coordination number of Ge is considered to be effective in forming covalent bonds and reducing the atomic diffusivity, which can provide sufficient amorphous stability *i.e.* the addition of third element will create compositional and configurational disorder in the material with respect to

the binary alloy, which will be useful in understanding the structural properties of these materials. Therefore, the structural studies of eutectic SbSe alloy doped by Ge with systematic compositional variation can be advantageous for gaining important insight in the structure-property relationships for these compounds.

Although, several reviews have appeared on various physical properties and applications of chalcogenide glasses [11-14], there is no thorough study of local atomic structure and its modification for eutectic SbSe alloy doped with Ge. Several experimental techniques such as X-ray diffraction (XRD), scanning electron microscopy (SEM) and Raman spectroscopy used to study the structure of chalcogenide alloys. Raman scattering is a very powerful experimental technique for providing information on the constituent structural units in a given material [15].

This paper presents some new results of a systematic study for eutectic Ge doped SbSe. XRD and Raman studies have been carried out to test the structure. Characterization of the basic parameters such as material density, average atomic volume, average coordination number, number of constraints and heat of atomization in dependence on composition, is also given.

2. Theoretical Basis

The densities of the pellets are determined from the relation,

$$\rho = \rho_l W_{air} / (W_{air} - W_l) \quad (1)$$

where W_{air} , W_l and ρ_l are, respectively, the weight of the sample in air, the weight of the sample in the liquid, and the density of the immersion liquid. Some physicochemical properties related to density were calculated in terms of the density and literature data [16-22] for each constituent element, summarized in **Table 1**.

The average atomic volume (V_a) was determined by the equation,

$$V_a = \frac{1}{\rho} \sum_i C_i A_i, \quad (2)$$

where A_i is the atomic weight of the i th component and C_i is the atomic concentration of the same element.

Structural properties of both amorphous and crystalline solids can be explained with topological models [23], chain crossing model (CCM) [24], random covalent network model (RCNM) [25] and chemical ordered network model (CONM) [26]. In these models, some of the properties can be discussed in terms of the average coordination number, which is indiscriminate of the species or valence bond. Average coordination number Z of a ternary $\text{Ge}_\alpha\text{Sb}_\beta\text{Se}_\gamma$ system is defined by the expression [27]:

$$Z = \frac{4\alpha + 3\beta + 2\gamma}{\alpha + \beta + \gamma} \quad (3)$$

where α , β , and γ are the atomic percentages of Ge, Sb and Se, while 4, 3, and 2 their coordination number. The coordination number Z characterizes the electronic properties of semiconducting materials, and shows the bonding character in the nearest-neighbor region [28].

The parameter R , which determines the deviation of stoichiometry and is expressed by the ratio of the covalent bonding possibilities of chalcogen atoms to that of non-chalcogen atoms, was calculated for a ternary $\text{Ge}_\alpha\text{Sb}_\beta\text{Se}_\gamma$ system using the following relation [29]:

$$R = \frac{2\gamma}{4\alpha + 3\beta} \quad (4)$$

The bond energies of various possible heteropolar Sb-Se, Se-Ge, and Sb-Ge bonds have been calculated on the basis of the relation postulated by Pauling [30]:

$$E_{A-B} = (E_{A-A}E_{B-B})^{0.5} + 30(X_A - X_B)^2 \quad (5)$$

Table 1. Literature data of the constituent elements in the synthesized alloys.

Property	Sb	Se	Ge
Density (g/cm^3)	5.30	4.28	5.00
Coordination number	3	2	4
H_s (kcal/g atom)	62.0	49.4	90.0
Bond energy (kcal/mol)	30.22	44.04	37.60
Electronegativity	2.05	2.55	2.01

where E_{A-A} and E_{B-B} are the single-bond energies and X_A and X_B are the electronegativities of atoms A and B , respectively.

For a ternary system $\text{Ge}_\alpha\text{Sb}_\beta\text{Se}_\gamma$, the average heat of atomization, H_s , can be determined as [31]:

$$H_s = (\alpha H_s^{\text{Ge}} + \beta H_s^{\text{Sb}} + \gamma H_s^{\text{Se}}) / (\alpha + \beta + \gamma) \quad (6)$$

where H_s is the heat of atomization of constituent atoms, and corresponds to the average nonpolar bond energy of the Ge-Ge, Sb-Sb and Se-Se chemical bonds [30]; α , β , and γ are the atomic percent of the corresponding elements. Calculations of these parameters are made on the basis of the density and composition measurements on these compounds.

3. Experimental

3.1. Sample Synthesis

The $\text{Sb}_{65}\text{Se}_{35-x}\text{Ge}_x$ ($x = 0, 5, 10, 15$ and 20 at%) bulk materials have been prepared according to the well established melt-quench technique. Appropriate atomic percentages of high purity elements (5 N) are vacuum sealed (10^{-5} Torr) into fused silica tubes of length 75 mm and internal diameter 8 mm. The sealed tubes are then heated in an electric furnace up to 850°C for 5 h. After complete melting and homogenization, the tubes are quenched in an ice-water mixture. The ingots were then ground into a fine powder with average particle size $<63 \mu\text{m}$. The main part of the as-quenched powder was used for preparation of powder compact disc shape samples (pellets) using the cold pressing technique. For this purpose a stainless steel die was used, where the forming pressure was adjusted to be 5 ton/cm^2 for all the prepared samples. The residual part of this powder was used for both SEM and XRD analyses.

3.2. The Characterization Properties of the Synthesized Samples

The characterization properties including structural, chemical compositions and density of Sb-Se-Ge system were measured. Various experimental techniques such as XRD, Raman, EDS and Archimedes methods were employed to study the samples at room temperature. The crystal structure of the synthesized alloys was determined by X-ray diffraction (XRD) using PANalytical X'PertPRO with Cu $K(\lambda = 1.5406 \text{ \AA})$ X-ray tube ($V = 40 \text{ kV}$, $I = 30 \text{ mA}$) with scanning speed $0.4^\circ/\text{S}$. The Raman spectra were obtained at room temperature using Perkin Elmer (Raman station 400) Raman spectrometer in the wavenumber region $500 - 80 \text{ cm}^{-1}$ at 4 cm^{-1} resolution and excitation wavelengths were provided by an Ar^+ Spectra-Physics Laser with exciting wavelength of 514.5 nm . The microstructure of the investigated samples were observed by field emission scanning electron microscope

(Joel JSM 7600F) combined with an energy dispersive spectroscopy (EDS) was used to do chemical analysis for specimens was measured using Archimedes balance method. The pellets used for density measurement were carefully chosen to be free from cracks and any surface contamination was removed by cleaning in methanol. For each composition the measurement was repeated four times and the obtained values were averaged. The accuracy of the density measurement, and consequently in average atomic volume (V_a) is estimated to be better than ± 0.01 . On the basis of the results obtained from the density and composition measurements, for each compound the average atomic volume (V_a), average coordination number (Z), parameter R and average heat of atomization (H_s) were determined using the above equations and presented in **Table 2**.

4. Results and Discussion

The compositional variation of density and average atomic volume (ρ and V_a versus x) of $\text{Sb}_{65}\text{Se}_{35-x}\text{Ge}_x$ alloys is shown in **Figure 1**. ρ and V_a show clear changes in slope at $x = 5$ ($\text{Sb}_{65}\text{Se}_{30}\text{Ge}_5$ composition). A sharp rise or decline from $x = 0$ to nearly 5 is followed by slightly changes above that composition. A similar fashion is also observed in the optical gap as Ge content increases [10]. Therefore, the effect of germanium on SbSe appears to be limited to composi-

tions with less than $x = 5$. This can be largely explained on the basis of chemical ordered network model (CONM) proposed by Biecerano and Ovshinsky [26]. In CONM, the glass structure is assumed to be composed of cross-linked structural units of the stable chemical compounds (heteropolar bonds) of the system and excess if any, of the elements (homopolar bonds). Due to the chemical ordering, features like extremum, a change in slope or kink [32], cur for the various properties at the tie line composition or the chemical threshold of the system. At this composition, the system structure is made up of cross-linked pyramidal-like SbSe_3 and tetrahedral-like GeSe_4 structural units which consist of the energetically favored heteropolar bonds only. Heteropolar bonds thus have pre-eminence over homopolar bonds and bonds are formed in the sequences of decreasing bond energy until all the available valences of the atoms are saturated. Each constituent is coordinated by $8-N$ atoms, where N is the number of electrons in outer shell and this is equivalent to neglecting the dangling bonds and the other valence defects. As can be seen from **Table 2**, a maximum in the compositional dependence of V_a is attained at $Z = 2.75$ which can be attributed to a change from two-dimensional (2D) layered structure to a three-dimensional (3D) network arrangement due to cross-linking. This Z value lies in the region near to Tanaka's threshold ($Z = 2.67$).

Table 2. Some physical parameters as a function of Ge content for $\text{Sb}_{65}\text{Se}_{35-x}\text{Ge}_x$ (where $x = 0 - 20$ at%) specimens.

Composition	ρ , $\text{g}\cdot\text{cm}^{-3}$	V_a	Z	Parameter R	H_s (kcal/g atom)	H_s/Z
$\text{Sb}_{65}\text{Se}_{35}$	5.96	17.92	2.65	0.36	57.59	21.73
$\text{Sb}_{65}\text{Se}_{30}\text{Ge}_5$	5.57	19.11	2.75	0.28	59.62	21.68
$\text{Sb}_{65}\text{Se}_{25}\text{Ge}_{10}$	5.95	17.84	2.85	0.21	61.65	21.63
$\text{Sb}_{65}\text{Se}_{20}\text{Ge}_{15}$	5.91	17.91	2.95	0.16	63.68	21.59
$\text{Sb}_{65}\text{Se}_{15}\text{Ge}_{20}$	6.08	17.35	3.05	0.11	65.71	21.54

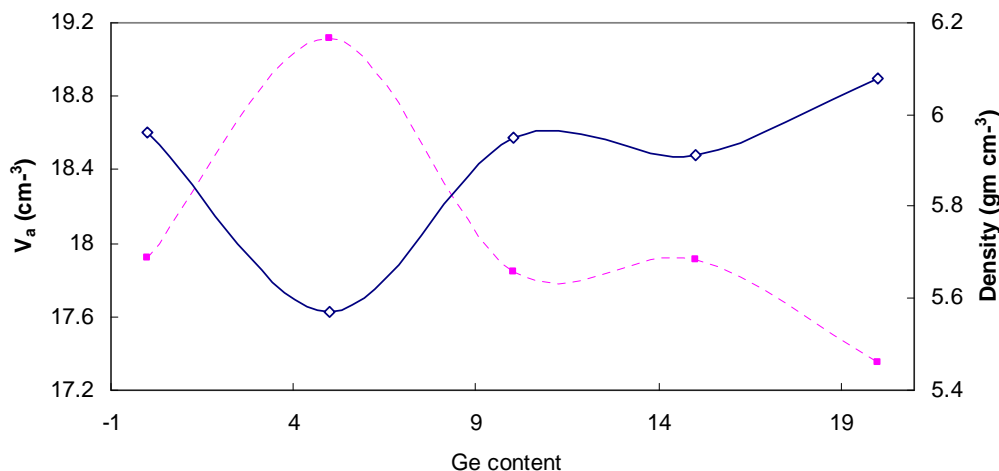


Figure 1. ρ and V_a versus Ge content

According to the constrain theory [33], the investigated compositions are over-coordinated, stressed-rigid and with lower connectivity, as the values of Z are larger than 2.4. These observations indicate that the effects of chemical ordering are also present in this system along with the overall topological effects. In other words, the dependence of V_a on Ge content and Z has been examined in light of topological and chemical ordered network models.

Other parameters, such as parameter R , also play an important role in the analysis of the results. Depending on R values, the chalcogenide systems can be organized into three different categories [29]:

1) For $R = 1$, the system reaches the stoichiometric composition since only hetero polar bonds are present.

2) For $R > 1$, the system is chalcogen-rich. There are hetero-polar bonds and chalcogen-chalcogen bonds present.

3) For $R < 1$, the system is chalcogen-poor. There are only hetero-polar bonds and metal-metal bonds present.

As shown in **Table 2**, values of R were found to be smaller than unity of the prepared system indicating Se-poor materials. There are only hetero-polar bonds and metal-metal (Sb-Sb) bonds present.

From the bonding energy values (**Table 3**) it follows that Ge-Se bonds with the highest possible energy are expected to be formed first, followed by Sb-Se bonds till saturation of all available valence of Se is achieved. There are still some unsaturated bonds of Sb, which must be bonded through formation of homopolar Sb-Sb bonds, being defects in the composition structure. In other words, the various bonds energies of expected bonds in the Sb-Se-Ge system are listed in **Table 3**. CONM could be applied to the present system. It allows the determination of the number of possible bonds and their type (heteropolar and homopolar). Therefore, only Sb-Se and Sb-Sb exist in the binary system consistent with CONM and R -values. Increasing the germanium content the amount of GeSe_4 tetrahedral unit increases at the expense of SbSe_3 pyramidal units, replacing the weaker Sb-Se bonds with the stronger Ge-Se ones.

The average heat of atomization (H_s) is a measure of the cohesive energy and it represents the relative bond strength, which in turn is correlated with the energy gap- of isostructural semiconductors. According to [34], for over-

constrained materials with higher connectivity ($3 \leq Z \leq 4$) the energy band gap depends much more strongly on H_s than for alloys with lower connectivity ($2 \leq Z \leq 3$). From **Table 2**, it can be seen that these alloys except $\text{Sb}_{65}\text{Se}_{15}\text{Ge}_{20}$ are with lower connectivity ($2 \leq Z \leq 3$) and the parameter H_s/Z is almost constant independently on composition. Therefore, the average heat of atomization H_s would have a negligible effect on the band gap energy values.

To identify the crystalline phases of the samples, X-ray diffraction was carried out for binary and ternary samples as shown in **Figure (2)**. Analysis of the X-ray diffraction pattern reveals that the diffraction peaks for the binary system ($\text{Sb}_{65}\text{Se}_{35}$ composition) correspond to the Sb_2Se rhombohedral phase. The unit cell contains nine layers stacked along the c -axis, five-layer stacks of Sb_2Se_3 and two-layer stacks of Sb_2 [35]. In the ternary composition, with increase in the Ge content, there is observed an up-shift to a higher value in the diffraction peaks with respect to those of the Sb_2Se crystalline phase. This indicates that the Ge is incorporated in lattice sites, perhaps substituting the Sb atoms as previously reported [36]. Also, the increase in the intensity of the main peak and the position of the peak shift can be attributed to the formation of GeSe_4 structural units with increasing Ge concentration.

Raman spectra were used to obtain basic structural information. For the vibrational bands reported in the literature for their crystalline accompaniment were taken as reference for the discussion of the spectrum [37-40]. The Raman spectra of $\text{Sb}_{65}\text{Se}_{35-x}\text{Ge}_x$ with $0 \leq x \leq 20$, depending on composition, are depicted in **Figure 3**. With no germanium substitution ($\text{Sb}_{65}\text{Se}_{35}$ composition), three characteristic vibrations were found at 98, 148 and 190 cm^{-1} , respectively. The first two bands are assigned to symmetrical pyramidal SbSe_3 bending modes. The band positioned at 190 cm^{-1} has been related to homopolar Sb-Sb in $\text{Se}_2\text{Sb-SbSe}_2$ structural units [37], due to the excess of antimony and Se-deficient system. This result is in excellent agreement with the value of R and CONM. It is interesting to note that the 192 cm^{-1} band is present, albeit quite weakly, even in the Raman spectrum of $\text{Sb}_{65}\text{Se}_{30}\text{Ge}_5$. This result is indicative of violation of the chemical order and the presence of a small concentration of Sb-Sb homopolar bonds in the structure of this composition. Moreover, the lowest frequency band and band at around 148 cm^{-1} , have intensities that strongly decrease with the progressive introduction of Ge to 5 at%, corresponding to GeSe_4 tetrahedra and SbSe_3 pyramids which are weakly coupled through two atomic -Se-Se bridging groups. This means that two bands could be the combined effect of the bending modes of Sb-pyramidal units and/or Ge-tetrahedral and addition of germanium until 5 at% causes a sharply

Table 3. Bond energies of various bonds in Ge-Se-Sb alloys.

Bond	Bond energy (kcal/mol)
Ge-Se	49.44
Sb-Se	43.98
Se-Se	44.04
Ge-Ge	37.60
Ge-Sb	33.76
Sb-Sb	30.22

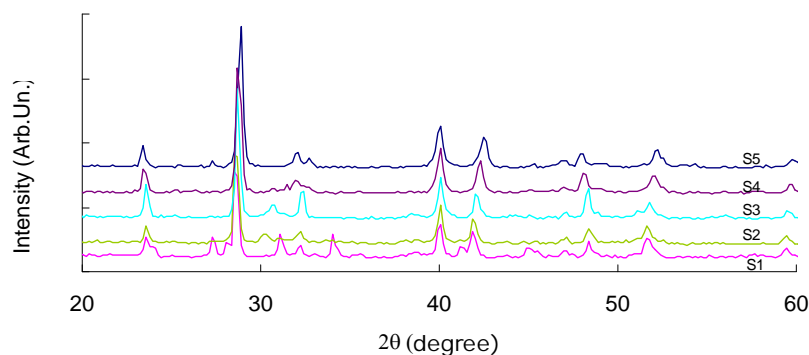


Figure 2. XRD patterns of S1) $\text{Sb}_{65}\text{Se}_{35}$, S2) $\text{Sb}_{65}\text{Se}_{30}\text{Ge}_5$, S3) $\text{Sb}_{65}\text{Se}_{25}\text{Ge}_{10}$, S4) $\text{Sb}_{65}\text{Se}_{20}\text{Ge}_{15}$, and S5) $\text{Sb}_{65}\text{Se}_{15}\text{Ge}_{20}$ alloys.

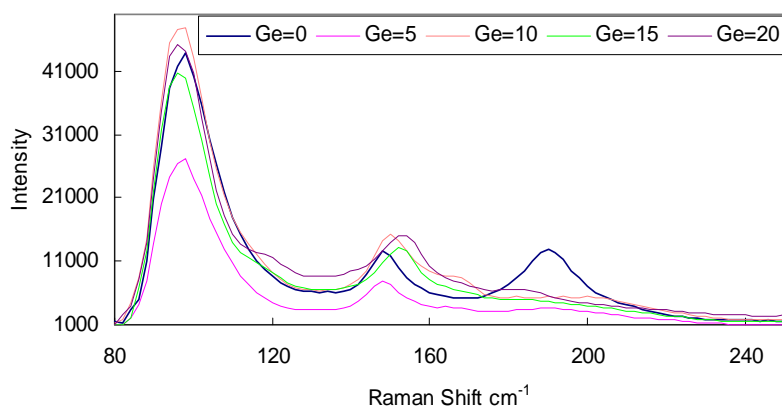


Figure 3. Raman spectra of all samples.

reduction in the intensity of the bands. However, the intensity of these bands decreases strongly when 5 at% Ge added to the binary system showing that the introduction of germanium leads to the decrease of the number of homopolar Sb-Sb bonds and increase the number of heteropolar Ge-Se bonds. Moreover, in addition to the main bands which appear at 96, and 150 cm^{-1} , a very broad, low intensity peak around 168 cm^{-1} is also observed for sample contained 10 at%. Band 168 cm^{-1} is assigned to Sb-Sb vibrations in $\text{Se}_2\text{Sb-SbSe}_2$ units [41]. At 15 at% Ge substitution, there are three bands located at 96, 152 and 168 cm^{-1} . In $\text{Sb}_{65}\text{Se}_{15}\text{Ge}_{20}$ alloy, bands 96, 154 and 184 cm^{-1} could be assumed to GeSe_4 tetrahedral and SbSe_3 pyramidal structural units.

Some important observations emerge from **Figure 3**:

1) For the binary system ($\text{Sb}_{65}\text{Se}_{35}$ composition), the vibrational spectra must correspond primarily to vibrational modes involving Sb-Se bonds as Se-Se bonds would be highly unexpected in these Se-poor materials and stretching modes of Sb-Sb homopolar bonds are located at significantly higher frequencies.

2) The vibrational spectra for Sb-Se-Ge system has been discussed by taking the formation of two basic structural units, SbSe_3 pyramids with three-fold coordi-

nated Sb atom at the apex and GeSe_4 tetrahedrons with Ge in the center.

3) A decrease in the peak height and an upshift to higher values may attribute to an increase in structural randomness [15].

4) By comparing peak position and Raman intensity in the range of bond modes, it is derived that the changes occur non-monotonically with increasing Ge content.

5. Conclusions

The chalcogenide bulk alloys with composition $\text{Sb}_{65}\text{Se}_{35-x}\text{Ge}_x$ ($x = 0 - 20$ at%) were prepared and characterized. From the measured composition and density of these materials the physical parameters (namely, ρ , V_a , Z , parameter R and H_s) have been evaluated. These parameters are well-correlated with topological and chemical ordered network models. All specimens are polycrystalline in nature as confirmed by XRD pattern. XRD and Raman spectroscopy were useful tools in the study of structural change induced by the progressive incorporation of Ge. The compositional dependence of the XRD and Raman spectra suggests the presence of two basic structural units, SbSe_3 pyramids with three-fold coordinated Sb atom at the apex and GeSe_4 tetrahedrons.

6. Acknowledgements

The authors express appreciation for the financial support to this work from the Deanship of Scientific Research, Najran University, Najran, Saudi Arabia, in the form of research project (Project No. NU 09/10).

REFERENCES

- [1] H. J. Borg, M. V. Shijndel, J. C. N. Rippers, M. H. R. Lankhorst, G. Zhou, M. J. Dekker, I. P. D. Ubbens and M. Kuijper, "Phase-Change Media for High-Numerical-Aperture and Blue-Wavelength Recording," *Japanese Journal of Applied Physics*, Vol. 40, No. 3B, 2001, pp. 1592-1597. [doi:10.1143/JJAP.40.1592](https://doi.org/10.1143/JJAP.40.1592)
- [2] P. K. Khulbe, T. Hurst, M. Horie and M. Mansuripur, "Crystallization Behavior of Ge-Doped Eutectic $Sb_{70}Te_{30}$ Films in Optical Disks," *Applied Optics*, Vol. 41, No. 29, 2002, pp. 6220-6229. [doi:10.1364/AO.41.006220](https://doi.org/10.1364/AO.41.006220)
- [3] N. Oomachi, S. Ashida, N. Nakamura, K. Yuso and K. Ichihara, "Recording Characteristics of Ge Doped Eutectic SbTe Phase Change Discs with Various Compositions and Its Potential for High Density Recording" *Japanese Journal of Applied Physics*, Vol. 41, No. 3B, 2002, pp. 1695-1697. [doi:10.1143/JJAP.41.1695](https://doi.org/10.1143/JJAP.41.1695)
- [4] M. H. R. Lankhorst, L. V. Pieterse, M. V. Shijndel, B. A. J. Jacobs and J. C. N. Rippers, "Prospects of Doped Sb-Te Phase-Change Materials for High-Speed Recording," *Japanese Journal of Applied Physics*, Vol. 42, No. 2B, 2003, pp. 863-868. [doi:10.1143/JJAP.42.863](https://doi.org/10.1143/JJAP.42.863)
- [5] Y.-C. Her and Y.-S. Hsu, "Optical Properties and Crystallization Characteristics of Ge-Doped $Sb_{70}Te_{30}$ Phase Change Recording Film," *Japanese Journal of Applied Physics*, Vol. 42, No. 2B, 2003, pp. 804-808. [doi:10.1143/JJAP.42.804](https://doi.org/10.1143/JJAP.42.804)
- [6] B. J. Kooia and J. T. M. De Hosson, "On the Crystallization of Thin Films Composed of $Sb_{3.6}Te$ with Ge for Rewritable Data Storage," *Japanese Journal of Applied Physics*, Vol. 95, No. 9, 2004, pp. 4714-4722.
- [7] T. Matsunaga and N. Yamada, "Crystallographic Studies on High-Speed Phase-Change Materials Used for Rewritable Optical Recording Disks," *Japanese Journal of Applied Physics*, Vol. 43, No. 7B, 2004, pp. 4704-4712. [doi:10.1143/JJAP.43.4704](https://doi.org/10.1143/JJAP.43.4704)
- [8] L. V. Pieterse, M. H. R. Lankhorst, M. V. Schijndel, A. E. T. Kuiper and J. H. J. Roosen, "Phase-Change Recording Materials with a Growth-Dominated Crystallization Mechanism: A Materials Overview," *Japanese Journal of Applied Physics*, Vol. 97, No. 8, 2005, pp. 083520-083527.
- [9] M. H. R. Lankhorst, B. W. S. M. M. Ketelaars and R. A. M. Wolters, "Low-Cost and Nano Scale Non-volatile Memory Concept for Future Silicon Chips," *Nature Mater*, Vol. 4, No. 4, April 2005, pp. 347-352. [doi:10.1038/nmat1350](https://doi.org/10.1038/nmat1350)
- [10] S. A. Saleh and A. Al-Hajry, "Optical Properties of Ge Doped Eutectic Sbse Thin Films," *Paper to be Presented in the 5th Meeting of the Saudi Physical Society (SPS5)*, Abha, October 2010, pp. 25-27.
- [11] A. Madan and M. P. Shaw, "The Physics and Applications of Amorphous Semiconductors," Boston, Massachusetts, 1988.
- [12] A. Feltz, "Amorphous Inorganic Materials and Glasses," Weinheim, Germany, 1993.
- [13] S. O. Kasap, "Handbook of Imaging Materials," 2nd Edition, Marcel Dekker, New York, 2002, p. 329.
- [14] K. Tanaka, "Encyclopedia of Materials," Elsevier, Oxford, 2001, p. 1123.
- [15] V. I. Mikla and V. V. Mikla, "Metastable States in Amorphous Chalcogenide Semiconductors," *Springer-Verlag, Berlin Heidelberg*, Vol. 128, 2010, p. 18. [doi:10.1007/978-3-642-02745-1](https://doi.org/10.1007/978-3-642-02745-1)
- [16] http://www.knovel.com/web/portal/periodic_table.
- [17] V. Pamukchieva and E. Savova, "Influence of Illumination on the Microhardness and Elastic Properties of Thin Gexsb40-Xs60 Films," *Thin Solid Films*, Vol. 347, No. 1-2, 1999, pp. 226-228. [doi:10.1016/S0040-6090\(99\)00017-6](https://doi.org/10.1016/S0040-6090(99)00017-6)
- [18] M. Fadel, "The Physical Properties and the Chemical Bond Approach for Se-Ge-As Amorphous Chalcogenide Glasses," *Vacuum*, Vol. 48, No. 1, 1997, pp. 73-83. [doi:10.1016/S0042-207X\(96\)00229-1](https://doi.org/10.1016/S0042-207X(96)00229-1)
- [19] J. Bicerano and S. R. Ovshinsky, "Chemical Bonding and the Nature of Glass Structure," Reidel Publishing Company, Holland, 1986.
- [20] Ambika and P. B. Barman, "Theoretical Prediction of Physical Parameters of Ge-Te-Bi Glassy Alloys," *Journals Ovonic Receives*, Vol. 3, No. 1, 2007, pp. 21-27.
- [21] <http://www.periodni.com/en/index.html>.
- [22] A. Dahshan and K. A. Aly, "Characterization of New Quaternary Chalcogenide As-Ge-Se-Sb Thin Films," *Philosophical Magazine*, Vol. 88, No. 3, 2008, pp. 361-372. [doi:10.1080/14786430701846214](https://doi.org/10.1080/14786430701846214)
- [23] J. C. Phillips, "Topology of Covalent Non-crystalline Solids I: Short-Range Order in Chalcogenide Alloys," *Journal of Non-Crystalline Solids*, Vol. 34, No. 2, 1979, pp. 153-181. [doi:10.1016/0022-3093\(79\)90033-4](https://doi.org/10.1016/0022-3093(79)90033-4)
- [24] P. Tronc, M. Bensoussan, A. Brenac and C. Sebenne, "Optical-Absorption Edge and Raman Scattering in GexSe1-x Glasses," *Physical Reviews B*, Vol. 8, No. 12-15, 1973, pp. 5947-5956. [doi:10.1103/PhysRevB.8.5947](https://doi.org/10.1103/PhysRevB.8.5947)
- [25] G. Lucovsky, F. L. Galeener, R. C. Keezer, R. H. Geils and H. A. Six, "Structural Interpretation of the Infrared and Raman Spectra of Glasses in the Alloy System Ge1-Xsx," *Physical Reviews B*, Vol. 10, No. 12, 1974, pp. 5134-5146. [doi:10.1103/PhysRevB.10.5134](https://doi.org/10.1103/PhysRevB.10.5134)
- [26] J. Bicerano and S. R. Ovshinsky, "Chemical Bond Approach to the Structures of Chalcogenide Glasses with Reversible Switching Properties," *Journal of Non-Crystalline Solids*, Vol. 74, No. 1, 1985, pp. 75-84. [doi:10.1016/0022-3093\(85\)90402-8](https://doi.org/10.1016/0022-3093(85)90402-8)

- [27] M. Yamaguchi, "The Relationship between Optical Gap and Chemical Composition in Chalcogenide Glasses," *Philosophical Magazine Part B*, Vol. 51, No. 6, 1985, pp. 651-663. [doi:10.1080/13642818508243153](https://doi.org/10.1080/13642818508243153)
- [28] A. F. Ioffe and A. R. Regel, "Semiconductivity in Pyrite, Marcasite and Arsenopyrite Phases," *Progress Semicond*, Vol. 4No. 239, 1960.
- [29] A. El-Korashy, *et al.* "Optical, Electrical and the Related Parameters of Amorphous Ge-Bi-Se Thin Films," *Physica B*, Vol. 365, 2005, pp. 55-64.
- [30] L. Pauling, "The Nature of the Chemical Bond," Cornell University Press, Ithaca, 1960.
- [31] V. Pamukchieva, *et al.*, "Compositional Dependence of the Optical Properties of New Quaternary Chalcogenide Glasses of Ge-Sb-(S,Te) System," *Optical Materials*, Vol. 32, No. 1, 2009, pp. 45-48. [doi:10.1016/j.optmat.2009.06.003](https://doi.org/10.1016/j.optmat.2009.06.003)
- [32] S. Mahadevan, A. Giridhar and A. K. Singh, "Studies on some Ge-Se-Te Glasses," *Journal of Non-crystalline Solids*, Vol. 103, No. 2-3, 1988, pp. 179-194. [doi:10.1016/0022-3093\(88\)90197-4](https://doi.org/10.1016/0022-3093(88)90197-4)
- [33] J. C. Phillips and M. F. Thorpe, "Constraint Theory, Vector Percolation and Glass Formation," *Solid State Commun*, Vol. 53, No. 8, 1985, pp. 699-702. [doi:10.1016/0038-1098\(85\)90381-3](https://doi.org/10.1016/0038-1098(85)90381-3)
- [34] M. Kastner, "Bonding Bands, Lone-Pair Bands, and Impurity States in Chalcogenide Semiconductors," *Physicals Review Letters*, Vol. 28, No. 6, 1972, pp. 355-357. [doi:10.1103/PhysRevLett.28.355](https://doi.org/10.1103/PhysRevLett.28.355)
- [35] V. Agafonov, N. Rodier, R. Ceolin, R. Bellissent, C. Bergman and J. P. Gaspard, "Structure of Sb_2Te_3 ," *Acta Crystallographica Section C*, Vol. 47, No. 6, 1991, pp. 1141-1143. [doi:10.1107/S0108270190013348](https://doi.org/10.1107/S0108270190013348)
- [36] E. Prokhorov, A. Mendoza-Galván, J. González-Hernández and B. Chao, "Effects of Ge Addition on the Optical and Electrical Properties of Eutectic $Sb_{70}Te_{30}$ Films," *Journal of Non-Crystalline Solids*, Vol. 353, No. 18-21, 2007, pp. 1870-1874. [doi:10.1016/j.jnoncrysol.2007.02.017](https://doi.org/10.1016/j.jnoncrysol.2007.02.017)
- [37] S. Sen, E. L. Gjersing and B. G. Aitken, "Physical Properties of $Ge_xAs_{2x}Te_{100-3x}$ Glasses and Raman Spectroscopic Analysis of Their Short-Range Structure," *Journal of Non-crystalline Solids*, Vol. 356, No. 41-42, 2010, pp. 2083-2088. [doi:10.1016/j.jnoncrysol.2010.08.013](https://doi.org/10.1016/j.jnoncrysol.2010.08.013)
- [38] P. Kumar, R. Thangaraj and T. S. Sathiaraj, "Effect of Sn Addition on the Optical Gap and Far-Infrared Reflectivity Spectra of Amorphous Sb-Se," *Journal of Non-Crystalline Solids*, Vol. 356, No. 31-32, 2010, pp. 1611-1613. [doi:10.1016/j.jnoncrysol.2010.05.046](https://doi.org/10.1016/j.jnoncrysol.2010.05.046)
- [39] L. Petit, *et al.*, "Effect of the Substitution of S for Se on the Structure of the Glasses in the System $Ge_{0.23}Sb_{0.07}S_{0.7-x}Se_x$," *Journals of Physics and Chemistry of Solids*, Vol. 66, No. 10, 2005, pp. 1788-1794. [doi:10.1016/j.jpics.2005.08.090](https://doi.org/10.1016/j.jpics.2005.08.090)
- [40] O. Kostadinova and S. N. Yannopoulos, "Raman Spectroscopic Study of Sb_xSe_{100-x} Phase-Separated Bulk Glasses," *Journal of Non-Crystalline Solids*, Vol. 355, No. 37-42, 2009, pp. 2040-2044.
- [41] J. Gutwirth, *et al.*, "Influence of Silver Concentration in $Ag_x(Sb_{0.33}S_{0.67})_{100-x}$ Thinamorphous Films on Photo-induced Crystallization," *Journal of Non-Crystalline Solids*, Vol. 353, No. 13-15, 2007, pp. 1431-1436. [doi:10.1016/j.jnoncrysol.2006.11.026](https://doi.org/10.1016/j.jnoncrysol.2006.11.026)